



ELSEVIER

Available online at [www.sciencedirect.com](http://www.sciencedirect.com)

SCIENCE @ DIRECT®

Tectonophysics 366 (2003) 165–185

TECTONOPHYSICS

[www.elsevier.com/locate/tecto](http://www.elsevier.com/locate/tecto)

# P-wave velocities of polymineralic rocks: comparison of theory and experiment and test of elastic mixture rules

Shaocheng Ji<sup>a,b,\*</sup>, Qin Wang<sup>b</sup>, Bin Xia<sup>a</sup>

<sup>a</sup>Guangzhou Institute of Geochemistry, Chinese Academy of Sciences, Wushan, Guangzhou 510640, PR China

<sup>b</sup>Département des Génies Civil, Géologique et des Mines, École Polytechnique de Montréal, C.P. 6079, Succursale Centre-Ville, Montréal, Québec, Canada H3C 3A7

Received 18 April 2002; accepted 11 March 2003

## Abstract

We compare the P-wave velocities ( $V_p$ ) of 696 dry samples measured at pressures up to 0.6–1.0 GPa with values calculated from the volume fraction and room pressure elastic constants of each constituent mineral using 16 averaging methods. The exceptional large number of samples covers almost all common lithologic types of igneous and metamorphic rocks. The calculated  $V_p$  data are in good agreement with laboratory values measured at about 300 MPa, even though elastic constants of only 22 common minerals are used in the computation. The mean  $V_p$  of a polymineralic rock is exclusively controlled by the volume fractions of its constituent minerals while grain shape and crystallographic preferred orientations, anisotropy and other perturbations have minimum effects. The mean  $V_p$  can be fairly well predicted as long as a relevant mixture rule is used and the volume fraction is accurately determined for each mineral. However, none of the mixture rules can simultaneously produce the best fit to measured P-wave velocities for all the lithologic types. One method may work well for one lithology but poor for other lithology. Even for a given lithology, an averaging method may yield good agreement at moderate pressure but poor agreement at high pressure. Applications of an inappropriate mixture rule will potentially cause the misinterpretation of the crust and mantle  $V_p$  data in terms of mineralogical compositions and structures.

© 2003 Elsevier Science B.V. All rights reserved.

**Keywords:** Elasticity of polymineralic rocks; P-wave velocities; Elastic mixture rules

## 1. Introduction

Whereas the upper crust is accessible to geological sampling, mapping, mining and drilling, the deeper portions of the crust and the whole mantle are relatively inaccessible. Much of our understanding about the

composition, structure and evolution of the deep crust and upper mantle has been derived from various seismic refraction and reflection measurements. Interpretation of these seismic data in terms of lithology, mineralogy and chemical composition is largely constrained by comparing in situ observed seismic velocities with those of relevant rocks or mineral assemblages thought to exist in the ranges of temperature and pressure of interest. Seismic velocities of rocks can be determined using two methods. The first is a direct laboratory measurement of available rock samples at elevated pressures (usually up to 0.6–1.0 GPa) and

\* Corresponding author. Département des Génies Civil, Géologique et des Mines, École Polytechnique de Montréal, C.P. 6079, Succursale Centre-Ville, Montréal, Québec, Canada H3C 3A7. Fax: +1-514-340-3970.

E-mail address: [sji@polymtl.ca](mailto:sji@polymtl.ca) (S. Ji).

the results are generally influenced by porosity, crack shape and distribution, compositional layering, anisotropy, alteration and secondary minerals. The alternation and secondary minerals, which formed during the exhumation, might not exist in the in situ rocks within the deep crust or upper mantle. The second method is a calculation of the overall magnitude of seismic velocities based on high-precision single crystal elastic constants and volume fractions of the constituent minerals of the rock and appropriate mixture rules. The mixture rules describe variations of effective elastic moduli of polymineralic composites as a function of their end-member elastic moduli and volume fractions (e.g., Watt et al., 1976; Ji and Wang, 1999). Seismic anisotropy of a rock can also be computed if the petrofabric data of its constituent minerals are available (e.g., Crosson and Lin, 1971; Baker and Carter, 1972; Mainprice, 1990). Calculated seismic properties are particularly useful in cases where samples are not available for measurement, as for instance, in modeling the crust and mantle velocities obtained from seismic inversion.

The elastic moduli ( $K$  and  $G$ ) of an isotropic polymineralic rock can be calculated from the elastic data of monomineralic aggregates of its forming minerals ( $M_i$ ) according to the generalized mean as follows:

$$M_c(t) = \left[ \sum_{i=1}^N (V_i M_i^t) \right]^{1/t} \quad (1)$$

where  $V_i$  and  $M_c$  are the volume fraction of  $i$ th mineral, and an overall elastic modulus (either  $K$  or  $G$ ) of the polymineralic rock consisting of  $N$  minerals, respectively, and  $t$  is a parameter. The case  $t=1$  yields the Voigt average ( $M_V$ ), and the case  $t=-1$  yields the Reuss average ( $M_R$ ). As  $t$  approaches 0, the limit of  $M_c(t)$  is the geometric mean ( $M_G$ ). It is noted that the  $M_G$  gives virtually identical results to the geometric means of the  $M_V$  and  $M_R$  bounds. Finally, the Hill or the Voigt–Reuss–Hill average of the overall elastic modulus ( $M_H$ ) is given by

$$M_H = \frac{1}{2} (M_V + M_R) \quad (2)$$

The subscripts V, R, H and G denote Voigt, Reuss, Hill and geometric averages, respectively.

The success of the elastic calculations depends on not only an accurate knowledge of the elastic properties

of the proposed minerals but also the adequacy of the mixture rule used. Although the approaches most frequently used for the elastic calculations are the Voigt, Reuss, Hill and geometric means, it has not been clear which mixture rule is the best to predict the average elastic properties of a given polymineralic rock. Crosson and Lin (1971) observed that the Voigt average from the room pressure elastic constants offers better predictions of  $V_p$  for the quasi-monomineralic Twin Sisters dunite (94.1% olivine, 4.9% orthopyroxene and 1% chromite and magnetite) than the other averages at pressures above 200 MPa. Seront et al. (1993) found that the Voigt average gives the closest approximation (within 0.1 km/s) to the high pressure (800 MPa) experimental  $V_p$  values of anorthosite (90% plagioclase and 10% olivine), while the Reuss and Hill schemes are significantly lower. The closest agreement between calculated and measured seismic velocities at 500–600 MPa has been reported for high-grade mylonites using the Voigt average (Siegesmund et al., 1989; Ji and Salisbury, 1993; Ji et al., 1993; Barruol and Kern, 1996). Thus, the Voigt average has been widely used in numerical modeling of rock seismic properties (e.g., Mainprice and Casey, 1990; Ji et al., 1994; Kern et al., 1996a,b, 2001; Saruwatari et al., 2001).

However, Christensen and Ramanantoandro (1971) and Babuska (1972) observed that the Hill average from the room pressure elastic constants provided the best prediction for the elastic wave velocities of dunite and bronzitite measured at 1.0 GPa. The Hill scheme was employed for calculating seismic properties of ultramafic rocks (Baker and Carter, 1972; Long and Christensen, 2000). Ji and Wang's (1999) experiments suggested that the shear-lag model, which gives lower P- and S-wave velocities even than the Reuss bound, should be more appropriate for hot-pressed olivine–orthopyroxene composites. Recently, Hurich et al. (2001) claimed that the Voigt average results in the least error between measured and calculated velocities at 400 MPa for granitic rocks while the Reuss average produces the best fit for gabbroic rocks.

In this study, we compare the measured  $V_p$  data of 696 dry samples with the theoretical values calculated using 16 different averaging models to search the relevant mixture rule which can yield the best estimation of overall seismic properties for each common type of polymineralic rocks in the crust and upper

mantle. We also try to verify if an averaging approach is good for a lithology but poor for other lithology and if the theoretical velocities calculated from the room pressure single crystal elastic constants and the volume fraction of the constituent minerals should be compared with the values measured at different pressures for different lithologies to obtain the closest agreement. An understanding of the influence of averaging schemes may lead to precise prediction of elastic wave velocities in polymineralic rocks. Such knowledge should also lead to better understanding the effects of lithology, porosity and mineralogy on the seismic properties of rocks, as well as to improv-

ing the geological interpretation of in situ seismic reflection and refraction data.

## 2. Procedure of Vp calculation

By neglecting its detailed microstructure (geometric orientation and distribution of each phase), a multiphase rock can be assumed to be macroscopically homogenous and isotropic, that is, their grains are equiaxed and have random crystal orientations. Such isotropic aggregates can be characterized by only two independent elastic constants (the bulk

Table 1  
Bulk ( $K$ ) and shear ( $G$ ) moduli (in GPa) of monomineralic aggregates calculated with the Voigt, Reuss, Hill and geometric averages

Mineral	Density	$K$ (Voigt)	$G$ (Voigt)	$K$ (Reuss)	$G$ (Reuss)	$K$ (Hill)	$G$ (Hill)	$K$ (Geometry)	$G$ (Geometry)
Apatite <sup>a</sup>	3.200	84.60	63.80	83.90	57.50	84.25	60.70	84.25	60.57
Calcite <sup>a</sup>	2.712	76.02	36.80	70.60	27.13	73.31	31.97	73.26	31.60
Clinopyroxene (Diopside) <sup>b</sup>	3.289	117.67	69.00	108.19	65.19	112.93	67.09	112.83	67.07
Epidote <sup>c</sup>	3.400	107.41	64.99	104.90	57.42	106.15	61.20	106.15	61.09
Garnet (Alm64Py22Gr1Sp11And2) <sup>d</sup>	4.131	176.83	95.90	176.83	95.88	176.83	95.89	176.83	95.89
Hornblende <sup>a</sup>	3.120	90.10	44.90	84.17	41.41	87.14	43.15	87.08	43.12
Ilmenite <sup>e</sup>	3.795	215.78	140.67	208.79	123.87	212.28	132.27	212.26	132.00
K-feldspar (Or78.5Ab19.4An2.1) <sup>a</sup>	2.560	62.66	31.85	44.80	22.61	53.73	27.23	52.98	26.83
Magnetite <sup>a</sup>	5.206	161.00	91.50	161.00	91.23	161.00	91.37	161.00	91.37
Mica (Muscovite) <sup>f</sup>	2.844	67.69	43.09	48.68	27.62	58.18	35.36	57.40	34.50
Olivine (Fo93Fa7) <sup>g</sup>	3.311	131.51	80.53	127.24	77.41	129.38	78.97	129.36	78.95
Omphacite <sup>h</sup>	3.327	133.50	80.64	127.96	77.69	130.73	79.16	130.70	79.15
Orthopyroxene (En80Fs20) <sup>i</sup>	3.354	104.79	75.51	102.13	73.92	103.46	74.72	103.45	74.71
Plagioclase (An29) <sup>a</sup>	2.640	66.42	33.71	59.58	29.09	63.00	31.40	62.91	31.32
Plagioclase (An53) <sup>a</sup>	2.680	73.83	35.82	67.52	31.31	70.68	33.56	70.60	33.49
Plagioclase (An9) <sup>a</sup>	2.610	57.53	32.70	44.07	25.79	50.80	29.25	50.35	29.04
Quartz <sup>a</sup>	2.648	38.12	47.60	37.56	40.98	37.84	44.29	37.84	44.17
Rutile <sup>a</sup>	4.260	217.33	124.60	208.57	98.65	212.95	111.63	212.91	110.87
Silimanite <sup>j</sup>	3.241	175.67	96.54	173.36	84.15	174.51	90.34	174.51	90.13
Spinel <sup>k</sup>	3.578	197.90	118.38	197.90	98.52	197.90	108.45	197.90	107.99
Zeolite (Natrolite) <sup>a</sup>	2.250	51.12	29.23	46.65	25.58	48.89	27.41	48.84	27.35
Zircon <sup>a</sup>	4.649	230.41	119.31	225.12	98.14	227.77	108.72	227.75	108.21

<sup>a</sup> Hearmon (1984).

<sup>b</sup> Levien et al. (1979).

<sup>c</sup> Ryzhova et al. (1966).

<sup>d</sup> Babuska et al. (1978).

<sup>e</sup> Weidner and Ito (1985).

<sup>f</sup> Vaughan and Guggenheim (1986).

<sup>g</sup> Kumazawa and Anderson (1969).

<sup>h</sup> Bhagat et al. (1992).

<sup>i</sup> Frisillo and Barsch (1972).

<sup>j</sup> Vaughan and Weidner (1978).

<sup>k</sup> Chang and Barsch (1973).

modulus  $K$  and the shear modulus  $G$ ). The Voigt and Reuss models are believed to represent the upper and lower bounds, respectively, on the actual overall elastic properties of a compacted aggregate. The Hill average has been widely used as the best representation of the overall elastic properties of polycrystalline aggregates (e.g., Watt, 1988; Zhao and Anderson, 1994); however, it does not give compatible stiffness ( $C_{ij}$ ) and compliance ( $S_{ij}$ ) tensors from a rigorous point of view. The compatibility between  $C_{ij}$  and  $S_{ij}$  is described by the following equation:

$$C_{ij}S_{ij} = I \quad (3)$$

where  $I$  is the unit tensor. This equation means that the ensemble average elastic stiffness  $C$  should equal the inverse of the ensemble average elastic compliances  $S$ . A geometric mean of the Voigt and Reuss bounds fulfills the compatibility described in Eq. (3) and is very close to the much more complicated iterative self-consistent micromechanical models (e.g., Matthies and Humbert, 1993; Mainprice and Humbert, 1994).

Owing to lack of information on the orientation of each individual grain, the study rock samples are assumed to be isotropic. Seismic velocities of such a polymineralic composite can be simply modeled according to a two-step procedure. The first step is involved calculating the elastic moduli ( $K_i$  and  $G_i$ ) of the polycrystalline monomineralic aggregate of  $i$ th constituent mineral from its elastic stiffness ( $C_{ij}$ ) and compliance ( $S_{ij}$ ) tensors. The second step is to calculate, using Eqs. (1) and (2), the overall elastic moduli ( $K$  and  $G$ ) of the sample according to its modal mineralogy ( $V_i$ ) and the results of the first step ( $K_i$  and  $G_i$ ). The resultant overall elastic moduli are then used to calculate P- and S-wave velocities of the sample. Both the steps involved Voigt, Reuss, Hill and geometric averaging approaches. Hence, there are in total 16 different approaches to calculate the overall elastic properties of a multiphase rock. They are inferred as VV, VR, VH, VG, RV, RR, RH, RG, HV, HR, HH, HG, GV, GR, GH and GG, where V, R, H and G denote the Voigt, Reuss, Hill and geometric averaging methods, respectively. The first letter signifies the averaging method used in the first step, and the second indicates the averaging method used in the second step. Unlike the complicated self-consistent method that needs to assume a specific microstructure

of the aggregate (e.g., Hill, 1965; Mainprice and Humbert, 1994), these simple averaging schemes are possible to predict the effective elastic properties of an isotropic polymineralic rock when only information on phase volume fraction is available.

In Table 1, we present the Voigt, Reuss, Hill and geometric averaging elastic properties of 22 common rock-forming minerals for zero-porosity, texture-free monomineralic aggregates at standard pressure and temperature (0.1 MPa and 25 °C), calculated from the elastic stiffness coefficients of these minerals using the methods described by Watt (1987).

### 3. Comparison of theory and experiment

#### 3.1. Measured $V_p$ data

The measured  $V_p$  data of totally 696 dry samples, which are compared with the calculated results, were carefully chosen from an internet-based database of rock seismic properties (DRSP, Ji et al., 2002a; also see Ji et al., 2002b). This database comprises almost all data available in the literature formally published in English and French during the last four decades and is more complete than previous compilations (e.g., Christensen, 1989; Schön, 1996). Such a computerized database, compared with a traditional compilation in the form of tables, can perform more complex tasks with higher speed and efficiency, and permit enormous volumes of data to be studied in a more comprehensive fashion than has hitherto been attempted. The DRSP can allow its user to retrieve P- and S-wave velocities and their anisotropy of rocks according to geographic location (country, province, region, longitude and latitude), tectonic province, rock category (igneous, metamorphic and sedimentary rocks and ores), lithology (granite, gabbro, eclogite, mylonite, sandstone, and many others), propagation and vibration directions ( $X$ —parallel to the stretching lineation,  $Y$ —perpendicular to the lineation and parallel to the foliation, and  $Z$ —normal to the foliation), strain (deformed or undeformed), humidity (dry or wet) and source literature. Almost all the experimental data used in this study are from credible laboratories such as those of N.I. Christensen, D.M. Fountain, H. Kern and M.H. Salisbury. Measurements in the laboratories of Christensen, Fountain, and Salisbury were

made on jacketed cylindrical samples in hydrostatic fluid-medium apparatus with transducers placed directly onto the sealed specimens (Christensen, 1985). Measurements in Kern's laboratory were performed on unjacketed, cube-shaped specimens in a cubic pressure apparatus. A state of nearly hydrostatic stress was achieved by pressing six pyramidal pistons in the three orthogonal directions onto the cubic samples (Kern, 1982). The velocities measured using both kinds of apparatus were calibrated to be accurate to 0.5–1.0% (Kern, 1982; Christensen, 1985).

The P-wave velocity used for the comparison with the calculated value of each sample is the arithmetic mean of the velocities measured from three mutually perpendicular directions. According to Christensen and Ramanantoandro (1971), the mean velocity calculated in this way gives a value very close to true isotropic elastic properties even in highly anisotropic rocks. For the rocks in which both foliation and lineation are developed, these directions are parallel to the *X*, *Y* and *Z* axes of the tectonic framework. If the sample is foliated but not lineated, both *X*- and *Y*-directions are arbitrarily aligned in the foliation plane. For samples that displayed neither foliation nor lineation, all the three directions are aligned in an arbitrary direction or only one direction is taken because such rocks are generally isotropic. All the  $V_p$  data selected for this study were measured on dry and low-porosity (<1%) samples at room temperature and confining pressures up to 0.6–1.0 GPa using the ultrasonic pulse transmission technique with frequencies of about 1–2 MHz (e.g., Birch, 1960; Kern, 1982; Christensen, 1985). The frequencies are higher than those used typically in the field investigations. As stated by Christensen (1989), however, dispersion in the frequency range between  $10^{-1}$  and  $10^7$  Hz is negligible, thus allowing direct use of the laboratory results in the interpretation of field seismic data.

As noted by many investigators, the velocity measured at low pressures during initial pressurization is commonly lower than the velocity measured during depressurization, due to the closing of microcracks at high pressures (Birch, 1960). Thus, only velocities obtained during depressurization are compared with the calculated values. Furthermore, the samples containing more than 5% minerals (e.g., serpentine, chlorite, sericite and talc), whose elastic stiffness coefficients are not available, were not used in the

comparison. These samples include mainly serpentinized peridotite and altered rocks.

The modal composition of each sample [ $V_i$  in Eq. (1)] was determined by microscopic image analysis (e.g., Barruol and Kern, 1996; Burlini et al., 1998) or standard point counting (e.g., Christensen, 1965; Ji et al., 1993; Fountain et al., 1994) on petrographic thin sections, or mass balance calculations from the chemical compositions of bulk rock and its constitutive minerals (e.g., Kern et al., 1996a,b). The modal composition data, which are critical for the accuracy of the  $V_p$  calculation (see Discussion), were obtained mainly from the point counting that is regarded to be accurate as long as the thin section can represent the bulk sample (Underwood, 1970). Either the  $V_p$  or modal composition data of the 696 samples studied are not tabulated here; they are available upon request from the authors.

### 3.2. Absolute error

The absolute error (Ae) between the calculated and measured velocities is defined as:

$$Ae(\%) = \frac{|V_c - V_m|}{V_m} \times 100\% \quad (4)$$

where  $V_c$  is the velocity calculated for the polymineralic rock at standard conditions (zero porosity, 0.1 MPa and 25 °C) using a given averaging approach, and  $V_m$  is the velocity measured at room temperature and a given pressure. The Ae value is taken as a statistic measure of the goodness of the prediction. The smaller the Ae, the better the agreement between the predicted and observed velocities.

Fig. 1, which was computed using data of all the 696 samples, illustrates the mean absolute error ( $\overline{Ae}$ ) versus pressure for each model. It is interesting to note:

- (1) The Hill averaging differs very little from the geometric mean. The Hill scheme is always slightly better than the geometric mean although the latter is more rigorous in the physical implication given in Eq. (1). The discrepancy of the VG from the VH, RG from RH, GV from HV, GH from HG, GR from HR, as well as GG from HH is in fact so small that it can be negligible (Fig. 1a).

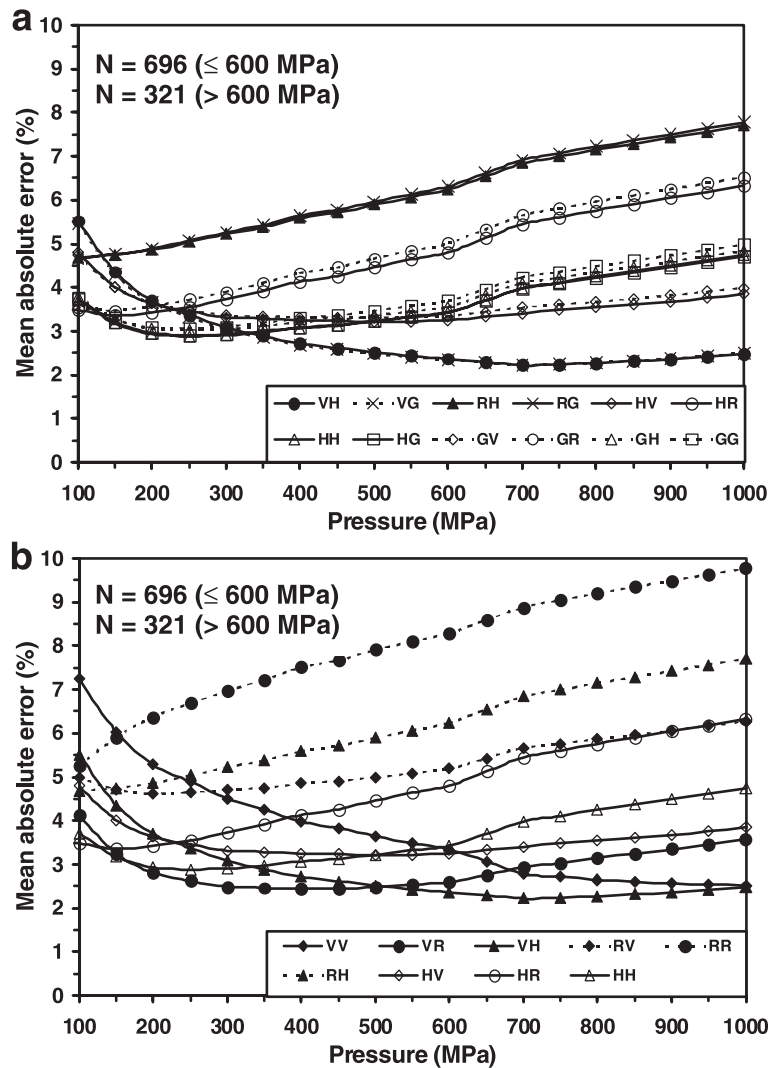


Fig. 1. Comparison of the theoretical P-wave velocities (zero porosity, 25 °C and 0.1 MPa) with those measured at different pressures. Mean absolute error ( $\bar{Ae}$ , %) is taken as a statistic measure of the goodness of each averaging model.  $N$ —sample number.

(2) The deviation of the  $V_p$  calculated according to the VV model from the measured value decreases with increasing pressure (Fig. 1b). The VV model gives a better estimate of  $V_p$  ( $\bar{Ae} < 3\%$ ) at pressures above 600–700 MPa. This is not surprising because seismic velocities almost always increase with increasing pressure and the VV represents theoretically the upper bound. A tendency is expected to decrease the deviation of the measured values at higher pressure from the VV bound calculated for the ideal, porosity-free aggregate from

the room pressure single crystal elastic constants (Fig. 2). This may be the reason for the common observation that the Voigt average exhibits a fairly good match to velocities measured at high pressures (Crosson and Lin, 1971; Seront et al., 1993; Ji et al., 1993; Ji and Salisbury, 1993; Kern et al., 1996a,b). In contrast, the RR model (lower bound) gives generally a poor prediction for the measured  $V_p$  value. The  $\bar{Ae}$  value of the RR model increases when the calculated  $V_p$  results are compared with the measurements at higher pressure.

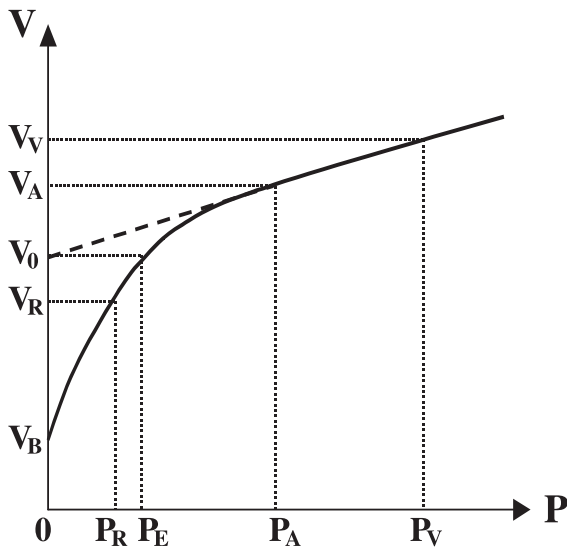


Fig. 2. Elastic wave velocity versus pressure.  $V_0$  is the projected 0.1 MPa pressure velocity;  $V_V$  and  $V_R$  are the theoretical velocities calculated using the Voigt and Reuss averages, respectively. Calculated  $V_V$ ,  $V_0$  and  $V_R$  should be compared with measured values at pressures  $P_V$ ,  $P_E$  and  $P_R$ , respectively, to obtain the best agreement.  $P_A$  is the critical pressure above which the rock can be considered as a compacted aggregate.

- (3) The VR and VH approximations yield the best estimate of  $V_p$  at pressures below and above 500 MPa, respectively (Fig. 1b). These two models thus offer a greater improvement over the HH, HV, HR, RV, RH, VV and RR models. The accuracy of these two models is within the current certainty of most in situ seismic measurements.
- (4) The calculated  $V_p$  values of the 696 samples according to the VR scheme at standard conditions display the best agreement with the measured data at about 300 MPa (Fig. 1b). It is well known that the  $V_p$ -pressure curves for rock samples (Fig. 2) are characterized by an initial quick, nonlinear rise in velocity below a critical confining pressure ( $P_A$ ), followed by a more gradual linear increase above this critical pressure (e.g., Christensen, 1965; Kern, 1982; Fountain et al., 1990; Ji et al., 1993). The linear rise indicates an elastic volume deformation of the compacted aggregates while the nonlinear rise marks a combination of the progressive closing of cracks and pore spaces (Birch, 1960; Christensen, 1965)

and lattice compression within the sample. As shown in Fig. 2,  $V_B$  and  $V_A$  are, respectively, the velocities measured at room pressure and at  $P_A$ , and  $V_0$  is the room pressure velocity, which is obtained from the extrapolation of the observed linear velocity–pressure relationship to room pressure.  $V_0 - V_B$  reflects the increase in velocity due to the closing of cracks and pore spaces while  $V_A - V_0$  corresponds to the velocity rise from the lattice compression. The present results suggest that the velocity measured at around 300 MPa ( $P_E$ ) statistically corresponds to the  $V_0$ .  $P_E$  may depend on lithology. It is noted that  $P_E$  is significantly lower for calcite-rich rocks than for silicate rocks. Because  $V_0$  is lower than  $V_A$  but higher than  $V_B$ , the  $P_A$  should be significantly higher than 300 MPa for most polyminerals rocks.

Among the 696 samples, 321 were measured up to 1.0 GPa and 375 up to 600 MPa. It is interesting to note that the general trend illustrated in Fig. 1 does not vary with the number of considered samples. The 696 samples have been classified into 15 lithologic types according to their chemical and mineral modal compositions, textures, and other information given in the original references (summarized in Ji et al., 2002a,b). Fig. 3 was built to verify if the general trend shown in Fig. 1b is applicable to each specific lithology. It is found that none of these averaging methods can simultaneously produce the best fit between the calculated and measured P-wave velocities for all the lithologic types. One method may work well for one lithology but poor for another lithology. In the range of 200–500 MPa, for example, the RH scheme gives the closest agreement with the measured  $V_p$  data for peridotite and eclogite (Fig. 3a–b) while the HH average is the best estimation for the  $V_p$  data for schist and intermediate gneiss/mylonite (Fig. 3c–d). For metasediment, gabbro-diorite, and mafic gneiss/mylonite, the HH and VR schemes fit almost equally well to the measured  $V_p$  data at 200–500 MPa (Fig. 3e–g). Even for a given lithology, an averaging method may yield good agreement at moderate pressure but poor agreement at high pressure. For pyroxenite, for example, the HV model is closest to the  $V_p$  data at 150–300 MPa while the VV model is better at >350 MPa (Fig. 3h). Granite–granodiorite (Fig. 3i),

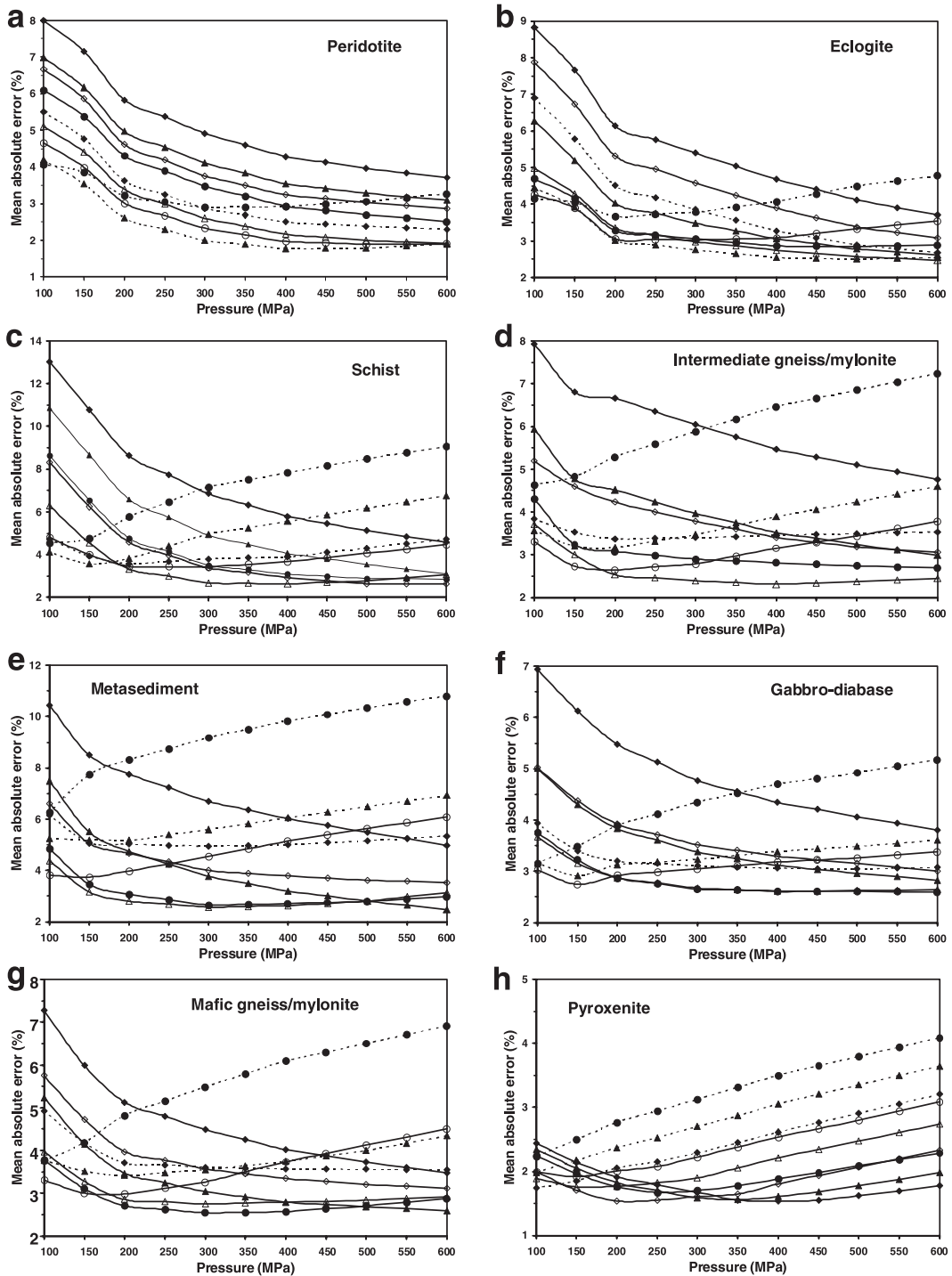


Fig. 3. Comparison of the theoretical P-wave velocities (zero porosity, 25 °C and 0.1 MPa) with those measured at different pressures for 15 common categories of rocks. Mean absolute error ( $\overline{Ae}$ , %) is taken as a statistic measure of the goodness of each averaging model.



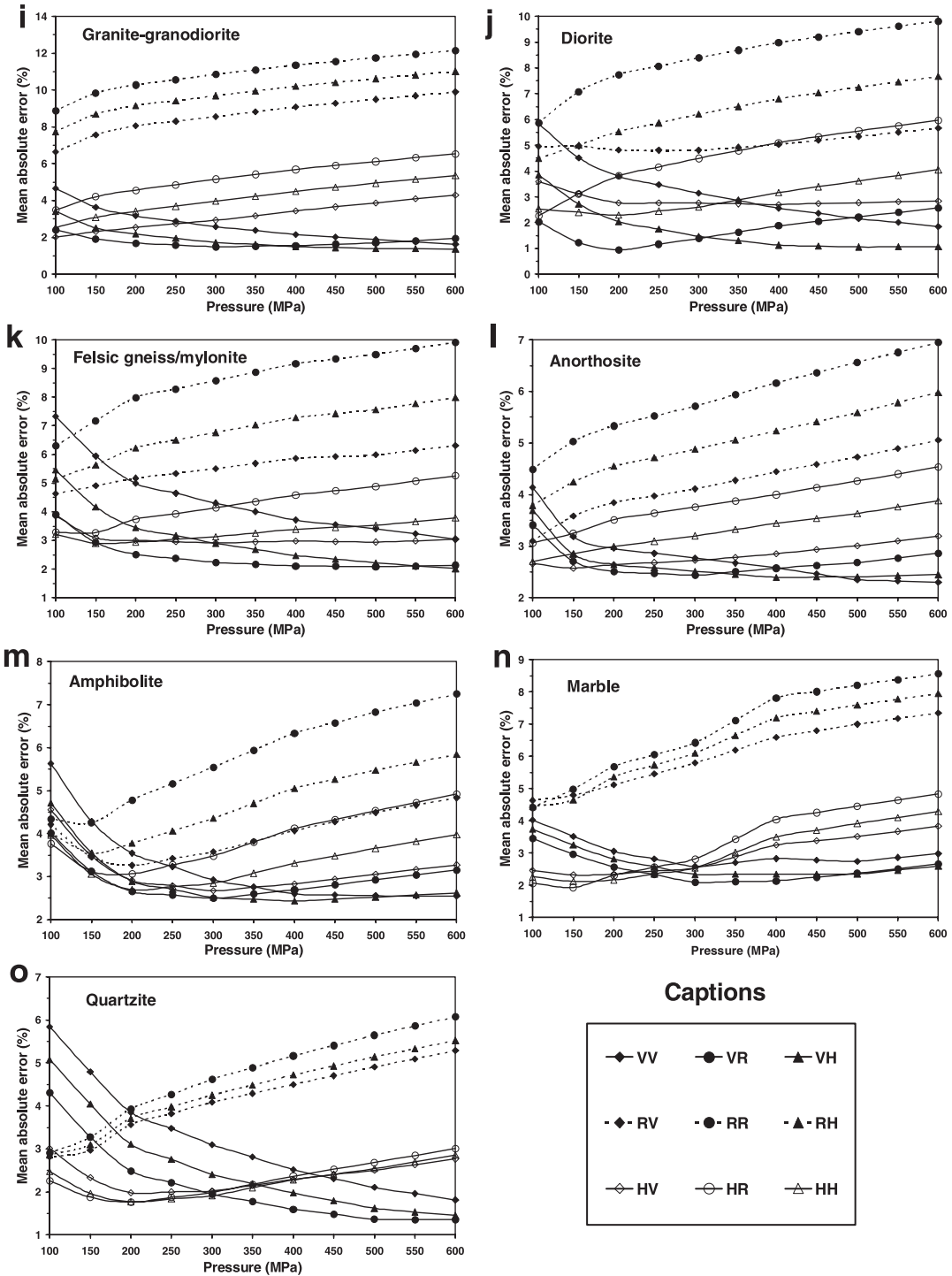


Fig. 3 (continued).

diorite (Fig. 3j), felsic gneiss/mylonite (Fig. 3k), anorthosite (Fig. 3l), amphibolite (Fig. 3m), marble (Fig. 3n) and quartzite (Fig. 3o) also fall into this category. The VR model is closest to the measured  $V_p$  data of granite–granodiorite below 400 MPa while the VH model does better above this pressure (Fig. 3i). For anorthosite, the best model is the VR, VH and VV models in the ranges of about 150–350, 350–500 and >500 MPa, respectively (Fig. 3l). For marble and quartzite, the VR does the best job of predicting the  $V_p$  values above 300 MPa while the HH does better below this pressure (Fig. 3n–o).

### 3.3. Relative error

The relative error (Re) between the calculated and measured velocities of each sample is defined as:

$$\text{Re}(\%) = \frac{V_c - V_m}{V_m} \times 100\% \quad (5)$$

Fig. 4 shows the distribution of Re for the VV, RR, HH, VR and GG models at 300 MPa. The measured P-wave velocities of 575 samples among a total of 696 samples lie in the range given by the VV upper and RR lower bounds. Eighty-one samples show their measured  $V_p$  slightly higher (mainly <2%) than the VV bounds (Fig. 4a). This phenomenon is observed in about 37% of amphibolites, 36% anorthosite, 33% pyroxenite, 25% marble, 21% diorite, 17% mafic gneiss/mylonite, 8% granite–granodiorite, felsic and intermediate gneiss/mylonite samples.

As shown in Fig. 4b, the RR average produces a systematic underestimation of the  $V_p$  values for common crustal igneous rocks (e.g., granite, granodiorite, anorthosite and gabbro–diabase) and metamorphic rocks (e.g., amphibolite, felsic, intermediate and mafic gneiss/mylonite, marble, quartzite, schist and metasediment). Forty samples among a total number of 696 have their  $V_p$  measured at 300 MPa lower than the RR bounds (Fig. 4b) and the “anomaly” occurs in 43% of peridotite, 30% eclogite, 9% pyroxenite, and 14% gabbro–diabase samples. For those rocks from the upper mantle, the measured velocities are lower than calculated values probably due to cracks that cannot completely close during experimental measurements at 300 MPa. These openings are believed to be the result of rapid tectonic exhumation from the upper mantle

depth to the surface, and can be fully closed only at high temperature and high pressure (e.g., >1.0 GPa, Christensen, 1965; Kern et al., 2001). In addition, the presence of a few percentages of alteration such as serpentine in peridotite and chlorite in eclogite and pyroxenite should tend to lower the measured velocities. A quantitative evaluation of the contribution of these impurities is difficult because their elastic stiffness coefficients have not been experimentally determined. Furthermore, recent high-pressure experiments on hot-pressed olivine–orthopyroxene mixtures (Ji and Wang, 1999) demonstrated that the measured velocity values are lower than the RR values, but can be better described by the shear-lag model that takes into account the mechanical interaction between phases.

It is interesting to note that the Re value of the HH or GG model shows an asymmetric distribution with respect to zero where the calculated  $V_p$  is exactly equal to the measured value (Fig. 4c and e), with the maximum in the domain of  $\text{Re} < 0$  or  $V_c < V_m$ . This indicates that both the HH (Fig. 5) and GG models tend to underestimate the  $V_p$  for the great majority of the samples. The VR model, however, displays a nearly normal distribution of Re with the maximum at zero (Fig. 4d). Such characteristic suggests that the VR model produces the best fit between the calculated and measured velocities at 300 MPa over all the 696 dry samples.

As demonstrated by the Re histograms in Fig. 5, the HH model tends to underestimate the  $V_p$  values of granite–granodiorite, diorite, felsic gneiss/mylonite, amphibolite, pyroxenite, anorthosite and marble, and to overestimate those of peridotite and eclogite at 300 MPa. Contrary to the suggestion of Hurich et al. (2001) that the HH average overestimates the velocity of gabbroic rocks, we observed that this averaging method produces statistically good agreement between the calculated and measured  $V_p$  values for gabbro–diabase and mafic gneiss/mylonite at 300 MPa (Fig. 5c–d). Moreover, it is also found that the HH model provides a fairly good match to  $V_p$  measured at 300 MPa for quartzite (Fig. 5l), schist (Fig. 5n), metasediment (Fig. 5o) and intermediate metamorphic rocks (Fig. 5f).

Fig. 6 shows the Re histograms for the VR model at 300 MPa. This model offers obviously an improvement over the other models for amphibolite, anortho-

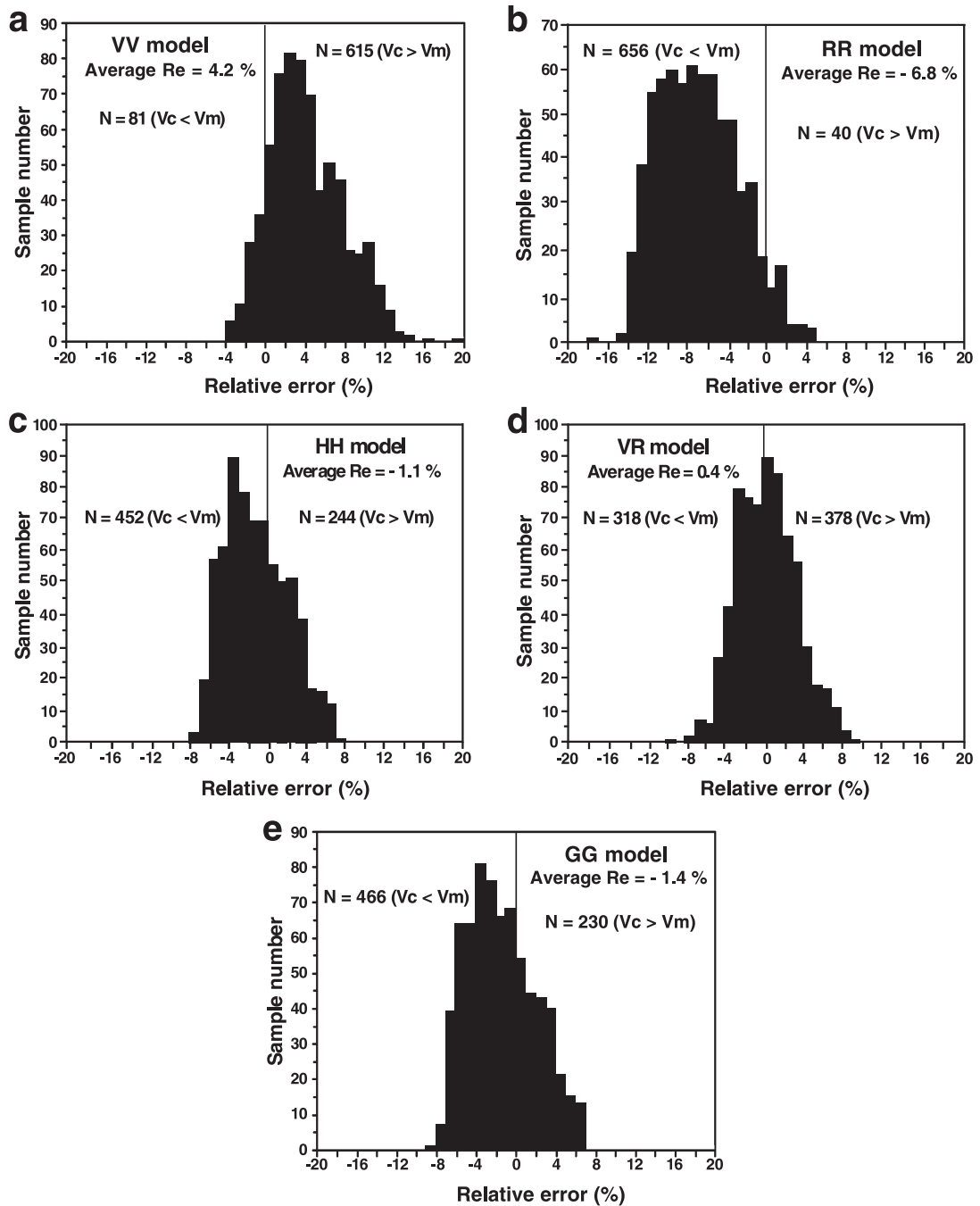


Fig. 4. Relative errors of the VV (a), RR (b), HH (c), VR (d) and GG (e) models for 696 samples. Calculated Vp data ( $V_c$ ) are compared with measured values ( $V_m$ ) at 300 MPa.  $N$ —sample number. The relative error is defined in Eq. (5).

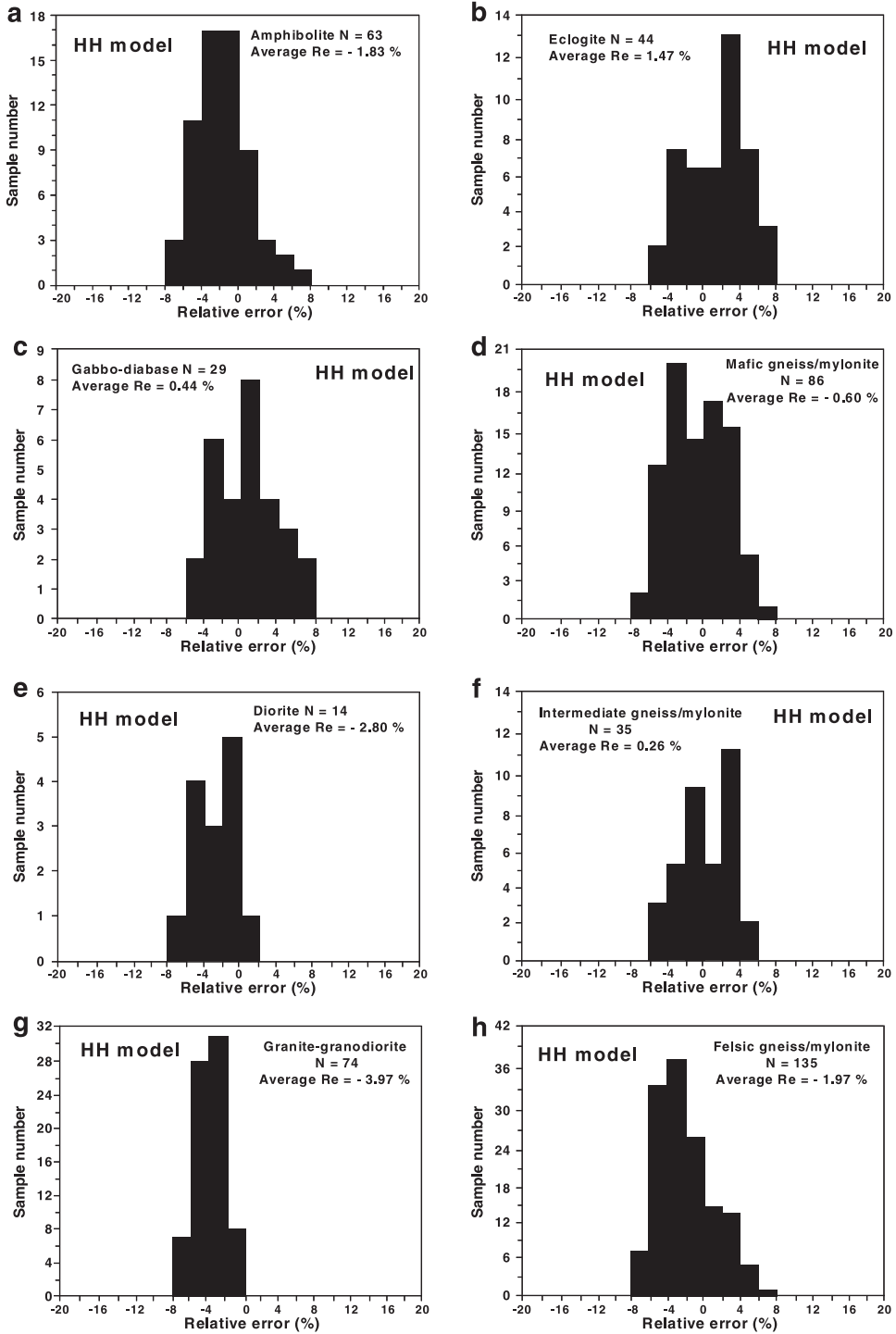


Fig. 5. Relative errors of the HH model for 15 common lithologic categories. Calculated Vp data are compared with measured values at 300 MPa. *N*—sample number. The relative error is defined in Eq. (5).

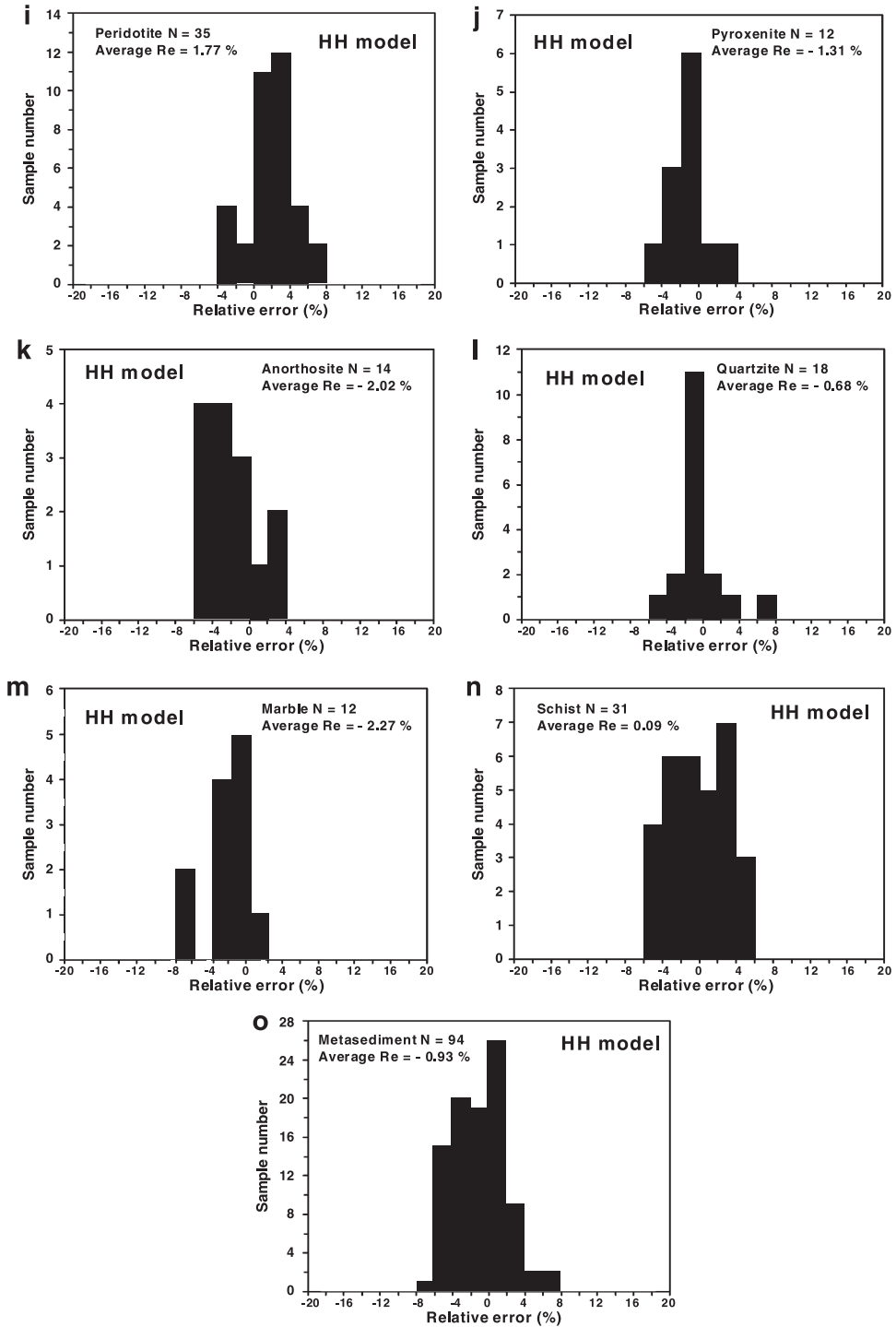


Fig. 5 (continued).

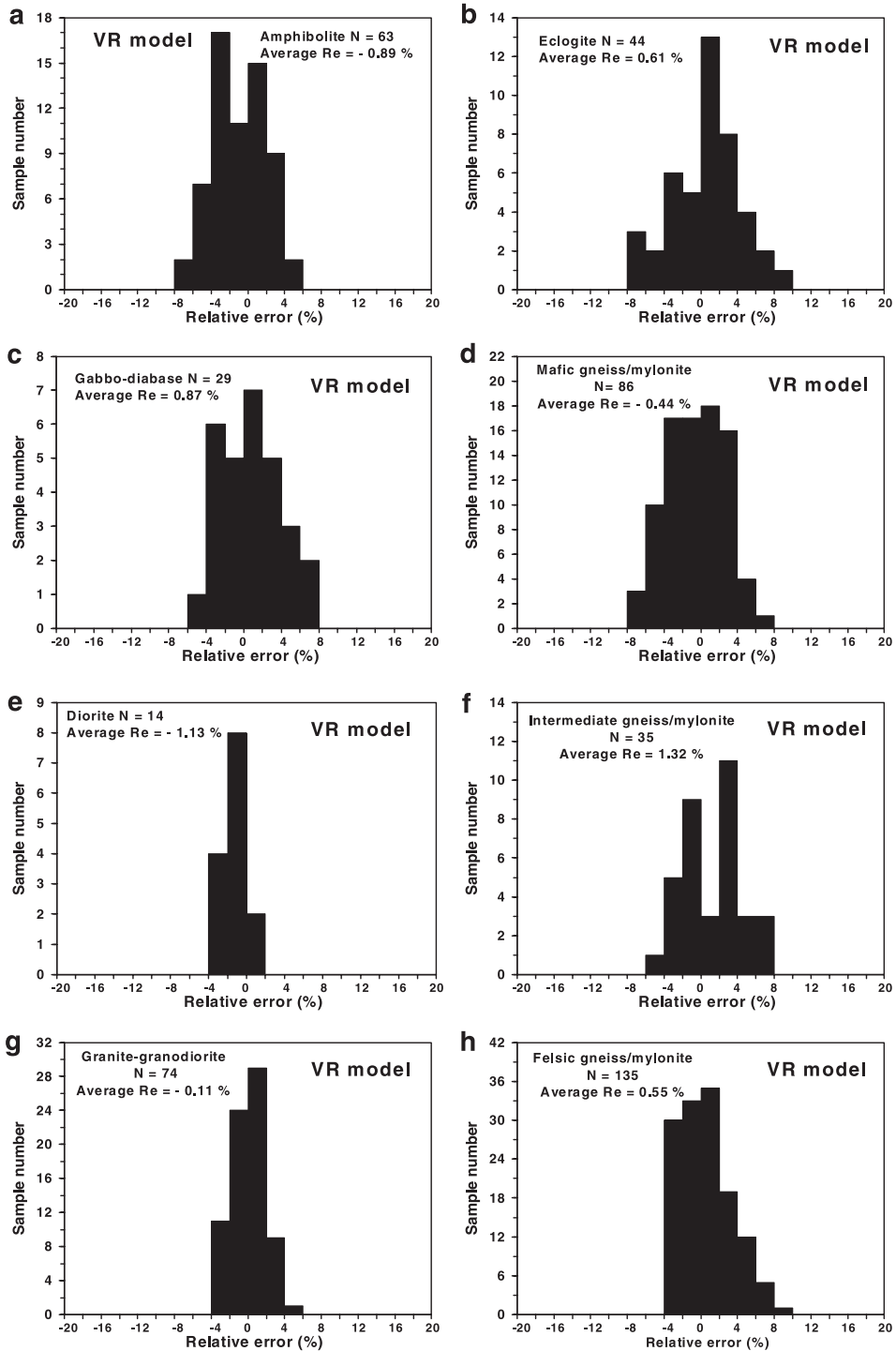


Fig. 6. Relative errors of the VR model for 15 common lithologic categories. Calculated Vp data are compared with measured values at 300 MPa.  $N$ —sample number. The relative error is defined in Eq. (5).

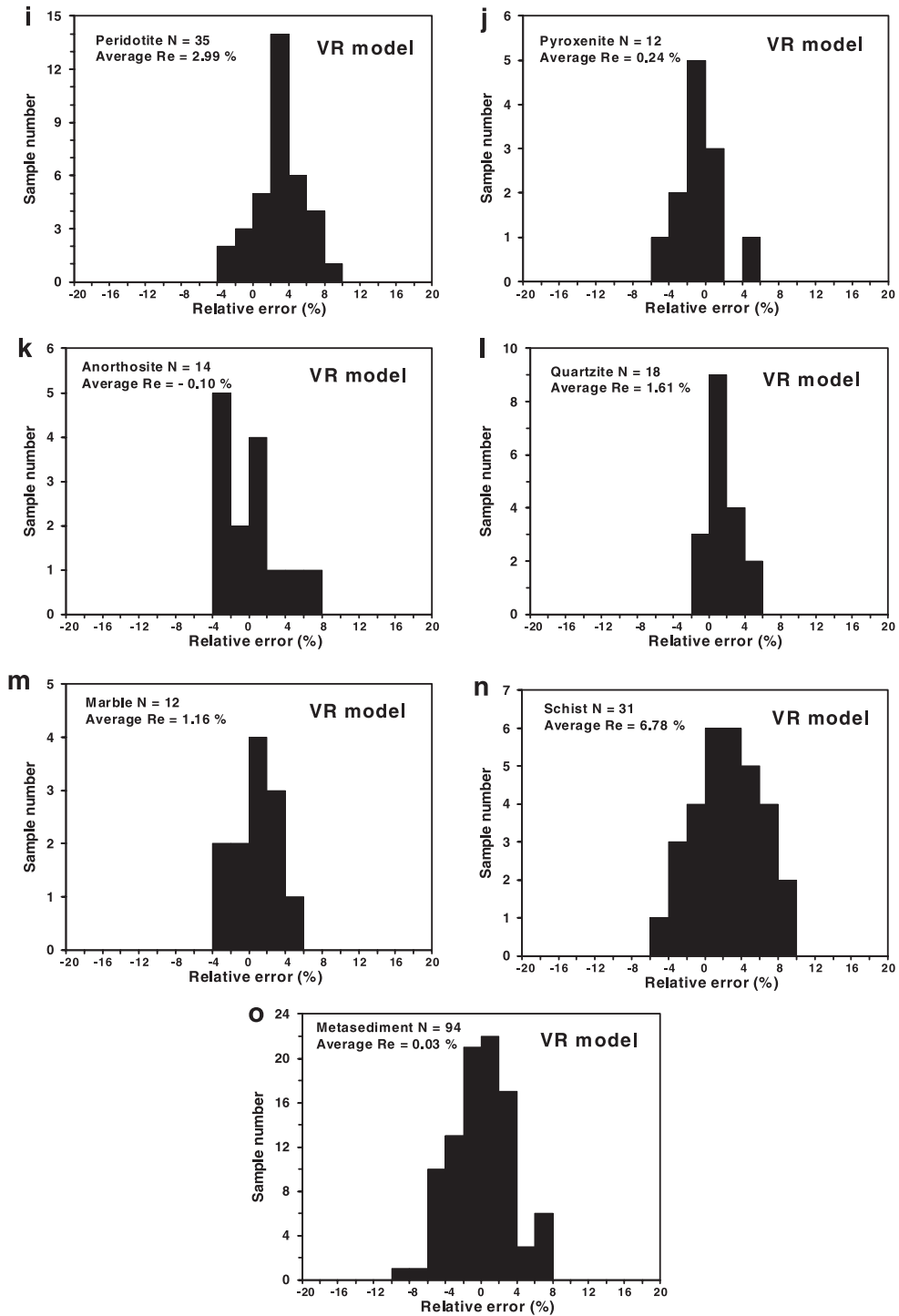


Fig. 6 (continued).

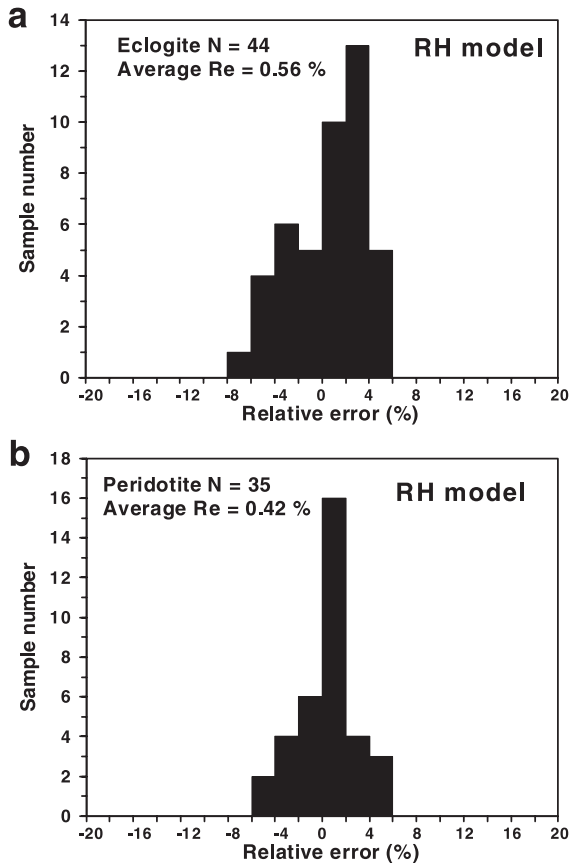


Fig. 7. Relative errors of the RH model for eclogite (a) and peridotite (b). Calculated  $V_p$  data are compared with measured values at 300 MPa.  $N$ —sample number. The relative error is defined in Eq. (5).

site, diorite, granite–granodiorite, felsic gneiss/mylonite and marble. For peridotite and eclogite, however, the RH gives the closest agreement to the measured  $V_p$  data (Figs. 4a–b and 7).

#### 4. Discussion

It is evident that the absolute errors of the calculated P-wave velocities are much larger than those arising from experimental errors in the measured values. The latter is estimated to be 0.5–1.0% (Kern, 1982; Christensen, 1985). We cannot discount the possibility that some errors in the input data for the calculations influence the comparison; however, the

source of such errors is undoubtedly difficult to avoid at this moment. Several possible causes are briefly analyzed below:

- (1) A constituent mineral with a complex chemical composition (e.g., amphibole, pyroxene, plagioclase and garnet) may not have exactly same elastic constants as the single crystal on which the published elastic constants were determined. It is likely that there are some minerals whose elastic constants are very similar to the rocks investigated while others not. It is unrealistic, if not impossible, to have elastic constants determined for each mineral of specific composition. Moreover, the single crystal elastic constants are determined on small crystals of gem quality, free of cracks or inclusions, which may be rare in natural rocks. In addition, grain boundaries are somewhat dirty and usually contain retrograde products. Effects of alteration and accessory minerals are difficult to evaluate because elastic constants of many alteration minerals (e.g., serpentine, sericite and chlorite) and accessory minerals are not available. We suggest, for want of accurate experimental data on single crystal elasticity of more minerals, that to use the elastic constants measured from a mineral having the closest composition to the component of the sample of interest should offer a significant improvement to the prediction of rock elastic properties.
- (2) The modal content data are obtained, using the standard point counting or image analysis techniques on a thin section, from a very small volume of each sample, as compared with the volumes of core or cubic samples in which velocities are measured. As long as compositional heterogeneity exists, the thin section may not be an accurate representation of the rock sample. It is interesting to note that errors in the modal content has less pronounced influence on  $V_p$  variations of felsic rocks than mafic rocks. This difference reflects the fact that  $V_p$  in potassium feldspar, plagioclase and quartz are very similar in felsic rocks while  $V_p$  in plagioclase, amphibole, garnet, clinopyroxene and orthopyroxene are considerably different in mafic rocks. As results, variations in the proportions of these minerals lead to very disparate  $V_p$  variations in mafic



rocks and metasediments while only a minor influence on seismic velocity of felsic rocks (e.g., Fountain et al., 1990).

- (3) Theoretically speaking, all the averaging approaches we use are applicable only to texture-free rocks in which neither shape preferred orientation (SPO) nor lattice preferred orientation (LPO) occurs. The developed SPO such as foliation and lineation generally result in a higher  $V_p$  parallel to the lineation while a lower  $V_p$  normal to the lineation (Seront et al., 1993; Ji et al., 1997). A LPO, if produced by a simple shear, is often of monoclinic symmetry with respect to the tectonic framework ( $X$ – $Y$ – $Z$ ) and may cause the fastest, intermediate and slowest P-wave velocities not exactly parallel to the  $X$ ,  $Y$  and  $Z$  directions (Ji et al., 1993). To check the potential effects of anisotropy on the comparison between the calculated and measured P-wave velocities, we plot the absolute error (Ae) against the seismic anisotropy for each sample (Fig. 8). The anisotropy is defined as  $100\% (V_{\max} - V_{\min})/V_{\text{mean}}$  (Birch, 1960). Table 2 lists the mean absolute error and mean anisotropy for the 15 main lithologic categories investigated. The absolute error, which is a statistic measure of the goodness of the comparison, shows no remarkable correlation with the seismic anisotropy. This indicates that the mean velocity calculated from the measurements in the  $X$ ,  $Y$  and  $Z$  directions does give a good approximation to true isotropic elastic properties even in highly anisotropic rocks. It also suggests that the goodness of the comparison between experiment and theory (i.e., HH, VR and VH models) depends mainly on the precision of mineral modal composition. Mainprice and Humbert (1994) observed that with increasing anisotropy, the separation between the Voigt and Reuss bounds increases, emphasizing the need for better methods. The mixed schemes such as VH and VR models, as suggested by the present study, appear to offer good empirical methods that allow some degree of compensation lying among the existing bounds.
- (4) Actually most of the observed departure of the calculated values from the measured values can be accounted for by the errors discussed above, although there are some systematic deviations that are likely caused by small but real differences

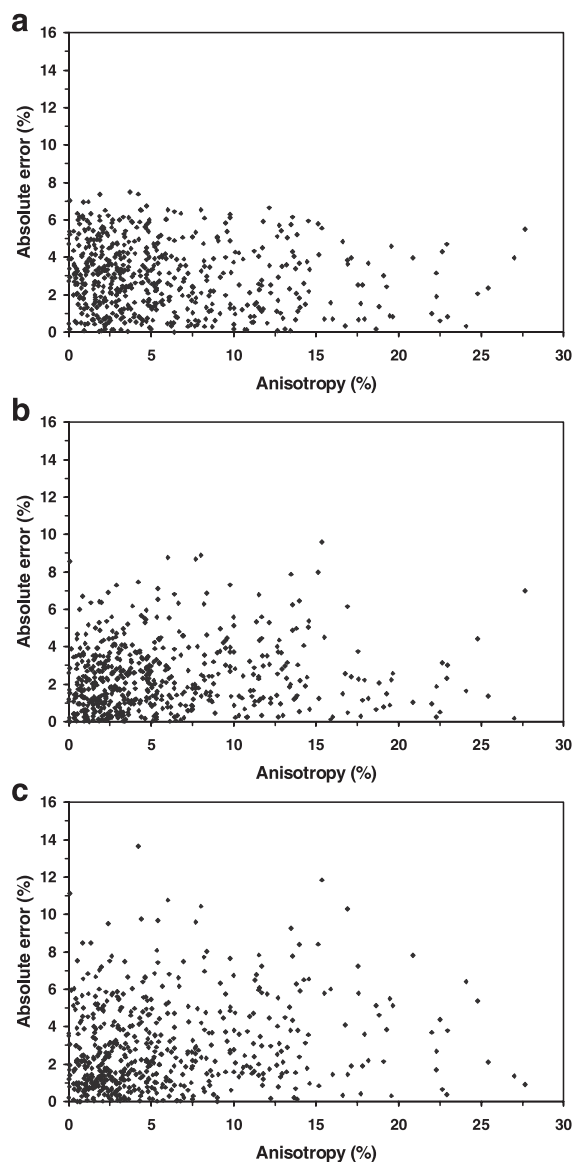


Fig. 8. Seismic anisotropy versus absolute error plots for each sample. (a) HH model, (b) VR model and (c) VH model. The absolute error is defined in Eq. (4). P-wave velocities and anisotropy were measured at 300 MPa.

between the ideal composites and measured samples. These systematic deviations are believed to relate to a mechanical interaction between minerals (Ji and Wang, 1999), a presence of residual stresses and effects of grain boundaries and interfaces that have a typical thickness of 0.1–

Table 2

Mean absolute error and mean seismic anisotropy for 15 common lithologic categories (the seismic velocities and anisotropy were measured at 300 MPa)

Lithology	Mean anisotropy (%)	Mean absolute error (%)		
		HH model	VR model	VH model
Anorthosite	2.2	3.1	2.7	2.7
Granite–granodiorite	2.3	4.1	1.5	1.6
Diorite	2.9	2.7	1.4	1.5
Gabbro–diabase	2.9	2.6	2.5	2.8
Eclogite	3.3	3.4	3.6	3.8
Pyroxenite	3.4	1.9	1.7	1.6
Mafic gneiss/ mylonite	3.9	2.7	2.5	2.8
Felsic gneiss/ mylonite	3.9	3.2	2.0	2.6
Intermediate gneiss/ mylonite	5.7	2.5	2.7	3.3
Peridotite	6.1	2.5	3.5	4.3
Marble	6.3	2.7	2.0	2.2
Quartzite	6.6	1.9	1.8	2.3
Amphibolite	9.2	2.8	2.5	2.4
Metasediment	10.8	2.6	2.5	3.6
Schist	13.6	2.7	3.7	4.9

1  $\mu\text{m}$  in natural rock samples. In a rock, the grains themselves act as perfectly elastic units while the contacts between grains—grain boundaries and interfaces—often display nonlinear elastic behaviour. As a result, the rock may be elastically nonlinear and hysteretic. The traditional theory of linear elasticity and resultant averaging methods thus may not do an accurate job of describing the overall elastic properties of these so-called nonlinear mesoscopic elastic materials (Guyer and Johnson, 1999).

In spite of the errors discussed above, the modal composition data generally lead to remarkably good prediction of the average  $V_p$  values in the studied 696 samples from quasi-isotropic (e.g., granite, granodiorite and diorite) to highly anisotropic (e.g., amphibolite, metasediment and schist) rocks. This seems to justify the assumption made, that a polymineralic rock could be regarded as an isotropic aggregate for analysis of its mean elastic properties and seismic wave velocities. It furthermore appears that the P-wave velocity of a polymineralic silicate rock at above 300 MPa can be fairly well predicted as long as the volume fractions and single crystal elastic constants of its constituent min-

erals are available and a relevant mixture rule is used. Therefore, the volume fractions of the rock-forming minerals are the critical factor in controlling the mean P-wave velocity of a polymineralic rock while grain shape and preferred orientation, anisotropy and other perturbations appear to have minimum effect on it. In other words, the deviation of the predicted values from the measured values is mainly due to errors in the determination of mineral volume fractions and to compositional heterogeneity of the rocks.

Similar to the Hill scheme, physical implications of the mixed averaging schemes such as VR, VH and RH remain unclear yet. However, we do find that the VR and VH schemes yield better agreements with experimental data than the VV, RR, HH and GG models below and above 500 MPa, respectively (Fig. 1). This may indicate that the Voigt average is relevant for monomineralic aggregates while the Reuss or Hill average is good for polymineralic composites. In fact, the mechanical processes in monomineralic aggregates (like-phase mixing) and in polymineralic composites (unlike-phase mixing) are generally different. For example, the stress transfer across a grain boundary between two like-phase grains is distinct from an interface between two unlike phases (Clyne and Withers, 1993). Thus, the detailed physical implication of each averaging scheme should be an important topic for future investigation.

As the uncertainties discussed above are difficult to avoid in the case of natural samples, comparisons between calculated and observed values of hot-pressed, isotropic multiphase composites with well-controlled chemical composition, volume fraction and geometric configuration of each phase are clearly preferable to better test the mixture rules (Watt et al., 1976; Zhang et al., 1996; Ji and Wang, 1999). Much work remains to be done in this area because it can yield better constraints on the interpretation of seismic data.

## 5. Conclusions

The following conclusions have been reached from the present study:

- (1) Application of the averaging methods to 696 dry samples for which both P-wave velocity and mineral modal composition were measured pro-

duced somewhat surprising results. The exceptional large number of samples covers almost all common lithologic types of igneous and metamorphic rocks. The seismic velocities calculated from the room-pressure single-crystal elastic constants are in good agreement with laboratory values measured at about 300 MPa, even though elastic constants of only 22 common minerals (Table 1) were taken into account in the computation. As long as a relevant averaging scheme is used and the volume fraction is correctly determined for each mineral, the calculated seismic velocities of most crustal and upper mantle rocks are certainly of quality high enough to characterize the average seismic properties of rocks, for example, for interpretation of seismic reflection and refraction profiles.

- (2) In the moderate pressure range (200–500 MPa), the RH average produced the best fit between the calculated and measured velocities for eclogite and peridotite. The HH average is the best estimation for the  $V_p$  data for schist and intermediate gneiss/mylonite. Either VR or HH is closest to the measured  $V_p$  data for metasediment, gabbro-diorite and mafic gneiss/mylonite at 200–500 MPa. The VV scheme fits best for pyroxenite at pressures above 350 MPa. For granite–granodiorite, diorite, amphibolite, anorthosite and felsic gneiss/mylonite, the VR average generally produces the best fit between the calculated and measured P-wave velocities at 200–300 MPa. At higher pressures, the VH or VG average is the best approximation of the measured values. For quartzite and marble, the VR scheme does the best job of predicting  $V_p$  values at above 250–300 MPa while the HH average does better at lower pressures. Hence, none of these averaging methods can simultaneously produce the best fit between the calculated and measured P-wave velocities for all the lithologic types or for the data at all different pressures. Applications of an inappropriate mixture rule should result in either under- or over-estimations for the mean  $V_p$  of a polymineralic rock in a given pressure range, depending on its lithology. Therefore, judicial selection of relevant mixture rule plays a critical role in the interpretation of the crust and mantle seismic data in terms of the mineralogical compositions and structures.

- (3) It is generally accepted that the geometric mean is satisfied with the rigorous physical condition that the aggregate mean is equal to the mean of the inverse property (i.e., mean elastic stiffness and compliance) while the Hill average lacks physical justification. The geometric mean, which was shown to be almost identical to the much more complicated iterative self-consistent method (Matthies and Humbert, 1993; Mainprice and Humbert, 1994), is actually very close to the Hill averaging at least for most of polymineralic rocks.
- (4) The goodness of the comparison between the calculated and measured  $V_p$  data shows no remarkable correlation with the seismic anisotropy, implying that the mean velocity calculated from the measurements in the  $X$ ,  $Y$  and  $Z$  directions represents a good approximation to bulk elastic properties of samples from quasi-isotropic (e.g., granite, granodiorite and diorite) to highly anisotropic (e.g., amphibolite, metasediment and schist) rocks.

### Acknowledgements

We thank the NSERC of Canada and LITHOPROBE for research grants. This is LITHOPROBE contribution no. 1299. S. Ji also thanks the Chinese Academy of Sciences and Guangzhou Institute of Geochemistry for a visiting professorship in 2002. We thank Dr. T. Popp, Dr. H. Thybo and an anonymous reviewer for critical reading of the manuscript.

### References

- Babuska, V., 1972. Elasticity and anisotropy of dunite and bronzite. *J. Geophys. Res.* 77, 6955–6965.
- Babuska, V., Fiala, J., Kumazawa, M., Ohno, I., Sumino, Y., 1978. Elastic properties of garnet solid solution series. *Phys. Earth Planet. Inter.* 16, 157–176.
- Baker, D.W., Carter, N.L., 1972. Seismic velocity anisotropy calculated for ultramafic minerals and aggregates. In: Heard, H., Borg, I., Carter, N.L., Raleigh, B. (Eds.), *Flow and Fracture of Rocks*. Monograph American Geophysics Union, pp. 157–166.
- Barruol, G., Kern, H., 1996. Seismic anisotropy and shear-wave splitting in lower-crustal and upper-mantle rocks from the Ivrea zone—experimental and calculated data. *Phys. Earth Planet. Inter.* 95, 175–194.
- Bhagat, S., Bass, J.D., Smyth, J., 1992. Single-crystal elastic prop-

- erties of omphacite-C2/c by Brillouin spectroscopy. *J. Geophys. Res.* 97, 6843–6848.
- Birch, F., 1960. The velocity of compressional waves in rocks to 10 kilobar, Part 1. *J. Geophys. Res.* 65, 1083–1102.
- Burlini, L., Marquer, D., Challandes, N., Mazzola, S., Zangarini, N., 1998. Seismic properties of highly strained marbles from the Splügenpass, central Alps. *J. Struct. Geol.* 20, 277–292.
- Chang, Z.P., Barsch, G.R., 1973. Pressure dependence of single crystal elastic constants and anharmonic properties of spinel. *J. Geophys. Res.* 78, 2418–2433.
- Christensen, N.I., 1965. Compressional wave velocities in metamorphic rocks at pressures to 10 kilobars. *J. Geophys. Res.* 70, 6147–6164.
- Christensen, N.I., 1985. Measurement of dynamic properties of rock at elevated temperatures and pressures. ASTM STP, vol. 869. American Society of Testing and Materials, Philadelphia, pp. 93–107.
- Christensen, N.I., 1989. Seismic velocities. In: Carmichael, R.S. (Ed.), *Practical Handbook of Physical Properties of Rocks and Minerals*, Section IV. CRC Press, Boca Raton, FL, USA, pp. 431–534.
- Christensen, N.I., Ramanantoandro, R., 1971. Elastic moduli and anisotropy of dunite to 10 kilobars. *J. Geophys. Res.* 76, 4003–4010.
- Clyne, T.W., Withers, P.J., 1993. *An Introduction to Metal Matrix Composites*. Cambridge Univ. Press, New York.
- Crosson, R.S., Lin, J.W., 1971. Voigt and Reuss prediction of anisotropic elasticity of olivine. *J. Geophys. Res.* 76, 570–578.
- Fountain, D.M., Salisbury, M.H., Percival, J., 1990. Seismic structure of the continental crust based on rock velocity measurements from the Kapuskasing uplift. *J. Geophys. Res.* 95, 1167–1186.
- Fountain, D.M., Boundy, T.M., Austrheim, H., Rey, P., 1994. Eclogite-facies shear zones—deep crustal reflectors. *Tectonophysics* 232, 411–424.
- Frisillo, A.L., Barsch, G.R., 1972. Measurements of single-crystal elastic constants of bronzite as a function of pressure and temperature. *J. Geophys. Res.* 77, 6360–6384.
- Guyer, R.A., Johnson, P.A., 1999. Nonlinear mesoscopic elasticity: evidence for a new class of materials. *Phys. Today*, 30–36 (April).
- Hearmon, R.F.S., 1984. The elastic constants of crystals and other anisotropic materials. In: Hellwege, K.H., Hellwege, A.M. (Eds.), *Landolt-Bornstein Tables*, III/18. Springer, Berlin, pp. 1–154.
- Hill, R., 1965. A self consistent mechanics of composite materials. *J. Mech. Phys. Solids* 13, 213–222.
- Hurich, C.A., Deemer, S.J., Indares, A., Salisbury, M., 2001. Compositional and metamorphic controls on velocity and reflectivity in the continental crust: an example from the Grenville Province of eastern Quebec. *J. Geophys. Res.* 106, 665–682.
- Ji, S., Salisbury, M.H., 1993. Shear-wave velocities, anisotropy and splitting in high-grade mylonites. *Tectonophysics* 221, 453–473.
- Ji, S., Wang, Z.C., 1999. Elastic properties of forsterite–enstatite composites up to 3.0 GPa. *J. Geodyn.* 28, 147–174.
- Ji, S., Salisbury, M.H., Hanmer, S., 1993. Petrofabric, P-wave anisotropy and seismic reflectivity of high-grade tectonites. *Tectonophysics* 222, 195–226.
- Ji, S., Zhao, X., Francis, D., 1994. Calibration of shear-wave splitting in the subcontinental upper mantle beneath active orogenic belts using ultramafic xenoliths from the Canadian Cordillera and Alaska. *Tectonophysics* 239, 1–27.
- Ji, S., Long, C., Martignole, J., Salisbury, M.H., 1997. Seismic reflectivity of a finely layered, granulite-facies ductile shear zone in the southern Grenville Province (Quebec). *Tectonophysics* 279, 113–133.
- Ji, S., Wang, Q., Salisbury, M.H., Schmitt, D., 2002a. Database of Rock Seismic Properties (DRSP), <http://texture.civil.polyuml.ca:8080/seismic-properties/index.jsp>.
- Ji, S., Wang, Q., Xia, B., 2002b. *Handbook of Seismic Properties of Minerals, Rocks and Ores*. Polytechnic International Press, Montreal. 630 pp.
- Kern, H., 1982. P- and S-wave velocities in crustal and mantle rocks under the simultaneous action of high confining pressure and high temperature and the effect of the rock microstructure. In: Schreyer, W. (Ed.), *High-Pressure Research in Geosciences*. E. Schweizerbart'sche Verlagsbuchhandlung, Stuttgart, pp. 15–45.
- Kern, H., Burlini, L., Ashchepkov, I.V., 1996a. Fabric-related seismic anisotropy in upper-mantle xenoliths: evidence from measurements and calculations. *Phys. Earth Planet. Inter.* 95, 195–209.
- Kern, H., Gao, S., Liu, Q.S., 1996b. Seismic properties and densities of middle and lower crustal rocks exposed along the North China Geoscience Transect. *Earth Planet. Sci. Lett.* 139, 439–455.
- Kern, H., Popp, T., Gorbatshevich, F., Zharikov, A., Lobanov, K.V., Smirnov, Y.P., 2001. Pressure and temperature dependence of Vp and Vs in rocks from the superdeep well and from surface analogues at Kola and the nature of velocity anisotropy. *Tectonophysics* 338, 113–134.
- Kumazawa, M., Anderson, O.L., 1969. Elastic moduli, pressure derivatives, and temperature derivatives of single-crystal olivine and single-crystal forsterite. *J. Geophys. Res.* 74, 5961–5972.
- Levien, L., Weidner, D.J., Prewitt, C.T., 1979. Elasticity of diopside. *Phys. Chem. Miner.* 4, 105–113.
- Long, C., Christensen, N.I., 2000. Seismic anisotropy of South African upper mantle xenoliths. *Earth Planet. Sci. Lett.* 179, 551–565.
- Mainprice, D., 1990. A FORTRAN program to calculate seismic anisotropy from the lattice preferred orientation of minerals. *Comput. Geosci.* 16, 385–393.
- Mainprice, D., Casey, M., 1990. The calculated seismic properties of quartz mylonites with typical fabrics: relationship to kinematics and temperature. *Geophys. J. Int.* 103, 599–608.
- Mainprice, D., Humbert, M., 1994. Methods of calculating petrophysical properties from lattice preferred orientation data. *Surv. Geophys.* 15, 575–592.
- Matthies, S., Humbert, M., 1993. The realization of the concept of a geometric mean for calculating physical constants of polycrystalline materials. *Phys. Status Solidi B* 177, K47–K50.
- Ryzhova, T.V., Aleksandrov, K.S., Korobkova, V.M., 1966. The elastic properties of rock-forming minerals: V. Additional data on silicates. *Izv. Earth Phys.* 2, 63–65.
- Saruwatari, K., Ji, S., Long, C., Salisbury, M., 2001. Seismic anisotropy of mantle xenoliths and constraints on upper mantle

- structure beneath the southern Canadian Cordillera. *Tectonophysics* 339, 403–426.
- Schön, J.H., 1996. *Physical Properties of Rocks*. Pergamon, New York. 583 pp.
- Seront, B., Mainprice, D., Christensen, N.I., 1993. A determination of the three-dimensional seismic properties of anorthosite: comparison between values calculated from the petrofabric and direct laboratory measurements. *J. Geophys. Res.* 98, 2209–2221.
- Siegesmund, S., Takeshita, T., Kern, H., 1989. Anisotropy of  $V_p$  and  $V_s$  in an amphibolite of the deeper crust and its relationship to the mineralogical, microstructural and textural characteristics of the rock. *Tectonophysics* 157, 25–38.
- Underwood, E.E., 1970. *Quantitative Stereology*. Addison-Wesley, Reading, MA.
- Vaughan, M.T., Guggenheim, S., 1986. Elasticity of muscovite and its relationship to crystal structure. *J. Geophys. Res.* 91, 4657–4664.
- Vaughan, M.T., Weidner, D.J., 1978. The relationship of elasticity and crystal structure in andalusite and sillimanite. *Phys. Chem. Miner.* 3, 133–144.
- Watt, J.P., 1987. POLYXSTAL: a Fortran program to calculate average elastic properties of minerals from single-crystal elasticity data. *Comput. Geosci.* 13, 441–462.
- Watt, J.P., 1988. Elastic properties of polycrystalline minerals: comparison of theory and experiments. *Phys. Chem. Miner.* 15, 579–587.
- Watt, J.P., Davies, G.F., O’Connell, R.J., 1976. The elastic properties of composite materials. *J. Geophys. Res.* 14, 541–563.
- Weidner, D.J., Ito, E., 1985. Elasticity of  $MgSiO_3$  in the ilmenite phase. *Phys. Earth Planet. Inter.* 40, 65–70.
- Zhang, M., Ebrom, D.A., McDonald, J.A., Tatham, R.H., 1996. Comparison of experimental velocity measurements with theoretical results in a solid–solid composite materials. *Geophysics* 61, 1429–1435.
- Zhao, Y., Anderson, D.L., 1994. Mineral physics constraints on the chemical composition of the earth’s lower mantle. *Phys. Earth Planet. Inter.* 85, 273–292.